Inflammation, Vol. 45, No. 2, April 2022 (© 2022)
https://doi.org/10.1007/s10753-021-01571-3

ORIGINAL ARTICLE

Simultaneous Modulation of NLRP3 Inflammasome and Nrf2/ARE Pathway Rescues Thioacetamide-Induced Hepatic Damage in Mice: Role of Oxidative Stress and Inflammation

Durgesh Kumar Dwivedi[1] and G. B. Jena[1,2]

Received 20 July 2021; accepted 21 September 2021

Abstract—— Chronic tissue injury resulting in fibrosis of multiple organs, responsible for one-third of the death globally. Liver fibrosis is a common pathway/condition involved in all chronic liver diseases. Thioacetamide (TAA), a hepatotoxicant, was used to induce hepatic fibrosis. Anti-diabetic drug glibenclamide (GLB) possesses anti-inflammatory properties and inhibits NACHT, LRR, and PYD domains-containing protein 3 (NLRP3) inflammasome activation. Dimethyl fumarate (DMF), a multiple sclerosis drug, activates the nuclear factor erythroid 2-related factor 2 (Nrf2)/antioxidant response element (ARE) pathway and maintains the antioxidant status in the cell. The present study was designed to investigate (i) role of NLRP3 inflammasome and Nrf2/ARE pathway in TAA-induced hepatotoxicity and liver fibrosis, (ii) mechanism involved in GLB and DMF mediated hepatoprotection against TAA-induced hepatotoxicity, and (iii) additional/synergistic hepatoprotective effect of combination treatment with NLRP3 inhibition + Nrf2 activation or GLB + DMF or MCC950 + 4OI to reverse/ameliorate the experimental liver fibrosis completely. TAA was administered intraperitoneally to mice for seven consecutive weeks, and treatments of GLB, DMF, GLB + DMF, MCC950, 4OI, and MCC950 + 4OI were provided for the last three consecutive weeks. The intervention with GLB, DMF, GLB + DMF, MCC950, 4OI, and MCC950 + 4OI significantly protected TAA-induced oxidative stress and inflammatory conditions by improving biochemical, histological, and immunoexpression changes in mice. The GLB, DMF, and GLB + DMF intervention exhibited a better protective effect compared with MCC950, 4OI, and MCC950 + 4OI, which revealed that this specific inhibitor/activator possesses only NLRP3 inflammasome inhibitory/Nrf2 activatory properties. In contrast, the clinical drug GLB and DMF have several other beneficial effects, which are independent of NLRP3 inhibition and Nrf2 activation.

KEY WORDS: liver fibrosis; thioacetamide; glibenclamide; dimethyl fumarate; MCC950; 4 octyl itaconate

[1]Facility for Risk Assessment and Intervention Studies, Department of Pharmacology and Toxicology, National Institute of Pharmaceutical Education and Research, Sector-67, S.A.S., Nagar, Punjab 160062, India
[2]To whom correspondence should be addressed at Facility for Risk Assessment and Intervention Studies, Department of Pharmacology and Toxicology, National Institute of Pharmaceutical Education and Research, Sector-67, S.A.S., Nagar, Punjab, 160062, India. Email: gbjena@niper.ac.in

INTRODUCTION

Globally, liver diseases are responsible for more than two million deaths annually [1]. According to a report published in The Lancet Journal Gastroenterology and Hepatology on cirrhosis by the global burden of disease (GBD) collaborators, 2017 estimated more than 1.32 million deaths occurred due to liver cirrhosis in 195 countries [2]. The etiologies include imbalanced diets, excessive alcohol consumption, viral infection, industrial exposure, and autoimmune disorders. Oxidative stress and inflammation are essential partners that present simultaneously and interact with each other, creating a vicious cycle to aggravate hepatic diseases, and mitigation of both oxidative stress and inflammation could be a successful strategy for protecting against liver injury. Chronic liver injury, persistent activation of inflammatory signaling, and sustained wound healing responses result in fibrogenesis. Fibrogenesis is a cellular and tissue process that drives progressive and excess deposition of extracellular matrix components, subsequently disrupting liver physiology. Thioacetamide (TAA) is a widely known hepatotoxicant used to induced liver fibrosis. These reactive metabolites covalently bind to cellular proteins and lipids and form adducts, which lead to alterations in the physiological functioning of hepatic parenchymal cells [3]. The mitochondria, peroxisomes, and microsomes in hepatocytes can produce reactive oxygen species (ROS), regulating on PPARα, which is mainly related to the hepatic fatty acid oxidation gene expression [4]. Under normal conditions, these physiologically generated ROS scavenged by endogenous antioxidant substances of cells. Dysregulation of the endogenous antioxidant system due to impaired physiological functioning arising from the TAA-mediated toxicity in hepatocytes results in excessive ROS production [4]. The prolonged and unregulated imbalance between the generation of free radicals and their elimination by endogenous antioxidant systems in the liver results in damage to crucial biomolecules of cells. During the repetitive hepatic injury, the infiltration of inflammatory cells, like lymphocytes, monocytes, and neutrophils, occurs at the injury site. This recruitment of inflammatory cells at the injury site further induces ROS production and upregulates the gene expressions of inflammatory mediators/substances. Oxidative stress generates various inflammatory cytokines such as TNF-α in Kupffer cells, which enhance inflammation and apoptosis in the liver [4]. Since these pathways modulate gene transcription, protein expression, cell apoptosis, and hepatic stellate cell activation, thereby oxidative stress and inflammation are considered as one of the pathological mechanisms that result in the initiation as well as the progression of chronic liver diseases. Thus, reducing oxidative stress and inflammation might be a successful strategy targeting hepatoprotection against chronic liver diseases.

Inflammasomes are the multimolecular protein complexes that initiate and perpetuate an inflammatory form of programmed cell death called pyroptosis. NLRP3 is one of the most characterized inflammasomes and has been well reported to upregulate in response to inflammatory stimuli. Recent evidence supports a key role of NLRP3 inflammasomes and their effectors in liver fibrogenesis and fibrosis development. Caspase-1 knockout mice have been reported to be protected from high-fat-diet-induced hepatic inflammation and fibrogenesis [5]. For the amelioration of inflammation, one of the most widely used anti-diabetic drugs, glibenclamide (GLB), was selected, which has already been reported to inhibit NLRP3 inflammasomes [6]. GLB mediated inhibition of NLRP3 inflammasomes has been well reported in several in vitro and in vivo experiments [7]. GLB has been reported to possess anti-inflammatory properties, as evidenced by the reduced secretion of IL-1β in diabetic mice [8], whereas Nrf2 is a transcription factor and is considered the master regulator of antioxidant status in cells. A tricyclic cyanoenone TBE-31 mediated Nrf2 activation in wild-type mice, reduced insulin resistance, decreased hepatic steatosis, and ameliorated NASH and suppressed liver fibrosis, but Nrf2-knockout mice showed obese and insulin resistance by long-term consumption of a high-fat high-fructose diet [9]. To overcome oxidative stress, an Nrf2 activator dimethyl fumarate (DMF) was chosen. DMF is a drug used for the treatment of a neurological disorder named multiple sclerosis. It has been reported to exhibit protective effects by activating the Nrf2 pathway in several experimental models such as pancreatitis, vascular injury, renal fibrosis, lung fibrosis, and hypertension [10].

MCC950 is a specific and selective NLRP3 inflammasome inhibitor, which blocks the release of IL-1β in LPS-primed and ATP/nigericin-activated macrophages in vitro [11]. Coll et al. reported that MCC950 did not directly inhibit NLRP3–ASC or NEK7–NLRP3

interaction, but it inhibits upstream signaling of the NLRP3 inflammasome [11]. It has been reported that oral intervention with MCC950 at the dose of 10 and 20 mg/kg for 8 weeks ameliorated liver levels of NLRP3, caspase-1, IL-1β, reduced plasma levels of IL-1β, IL-6, lowered ALT/AST, and suppressed the severity of liver inflammation as well as liver fibrosis in mice exposed to atherogenic diet or methionine-choline deficient diet [12]. In recent years, Green et al. reported that, like other chloride efflux inhibitors, MCC950 inhibits the formation of ASC specks [13]. Itaconate comprises an electrophilic compound that alkylates essential KEAP1 cysteine residues, which permits the aggregation of newly synthesized Nrf2. Subsequently, Nrf2 translocates to the nucleus, and the transcription of antioxidant and anti-inflammatory signaling cascade occurs [14]. 4-OI alkylates a number of KEAP1 cysteines (Cys) residues Cys151, Cys257, Cys288, Cys273, and Cys297. Cysteine 151 is the primary sensor on KEAP1 for DMF as well as other Nrf2 activator sulforaphane [14]. Tang et al. reported that treatment with 4OI inhibited high glucose-induced ROS and superoxide generation, lipid peroxidation, mitochondrial depolarization, death, and apoptosis of human umbilical vein endothelial cells [15].

Therefore, either the inhibition of the NLRP3 inflammasome or the activation of the Nrf2/ARE pathway could be a rational strategy for protection against liver diseases. Alone and a combination treatment of GLB and DMF were provided to check whether simultaneous modulating the NLRP3 and Nrf2 pathway could ameliorate the experimental chronic liver disease. Further, the hepatoprotective protective effect of test drugs (GLB and DMF) compared with specific NLRP3 inflammasome inhibitor (MCC950) and specific Nrf2 activator (4-octyl itaconate; 4OI). The present study was designed to investigate (i) role of NLRP3 inflammasome and Nrf2/ARE pathway in TAA-induced hepatotoxicity and liver fibrosis, (ii) mechanism involved in GLB and DMF mediated hepatoprotection against TAA-induced hepatotoxicity, (iii) compare hepatoprotective effect exhibited by GLB versus MCC950 (specifically inhibit NLRP3 inflammasome), DMF versus 4OI (specifically activate Nrf2), and (iv) additional/synergistic hepatoprotective effect of combination/concurrent treatment with NLRP3 inhibitor + Nrf2 activator or GLB + DMF or MCC950 + 4OI to completely reverse/ameliorate the experimental liver fibrosis completely.

MATERIALS AND METHOD

Animals

The Institutional Animal Ethics Committee approved the experimental animal protocols against approval number IAEC/19/15. Male BALB/c mice (18–22 g; 7–8 weeks old) were obtained from the Central Animal Facility (CAF) of our institute NIPER, SAS Nagar, Punjab. The environmental conditions such as relative humidity (40–70%), room temperature (20–26 °C), and 12-h light/dark cycle were constant during the period of the whole experiment. Normal/standard pellet diet and purified water were provided to animals ad libitum.

Chemicals

TAA (99%, CAS# 62–55-5), GLB (99%, CAS# 10238–21-8), DMF (99%, CAS# 624–49-7), carboxymethyl cellulose sodium salt (sodium CMC), and other general-purpose reagents were procured from Sigma-Aldrich Chemicals (St. Louis, MO, USA). MCC950 (> 97%, CAS# 256373–96-3) was purchased from Merck KGaA, Darmstadt, Germany. 4-octyl Itaconate (> 98%, CAS# 3133–16-2) was purchased from Cayman Chemical, Ann Arbor, MI, USA. Dimethyl sulfoxide, Hanks balanced salt solution, low and normal melting-point agarose, ethylenediaminetetraacetic acid disodium salt, and triton X-100 were purchased from Hi-Media Laboratories Ltd, Mumbai, Maharashtra, India.

Experimental Design and Rationality of Dose Selection

The treatments were provided as follows. Intraperitoneal TAA treatment at an escalating dose (50–400 mg/kg, thrice-weekly) for seven consecutive weeks, started with initial treatment with 50 mg/kg, as described by Kim et al., in the research topic titled "Optimized mouse models for liver fibrosis" [16]. The GLB dose 1 mg/kg and DMF and DMF dose 50 mg/kg were provided on the basis of literature as well as previous studies performed by the authors [17–20]. The protective dose of MCC950 at 10 mg/kg was selected on the basis of a literature report for the beneficial effects on the liver as well as other organs [21, 22]. The protective dose of 4OI at 50 mg/kg

was selected on the basis of a literature report for the beneficial effects on the liver and other organs [23, 24]. The interventions of oral GLB (1 mg/kg), oral DMF (50 mg/kg), MCC950 (10 mg/kg, ip), and 4OI (50 mg/kg) were provided for the last three consecutive weeks. The terminal body weight was taken on the last day before sacrifice. After sacrifice, the livers from mice were isolated, washed in chilled phosphate-buffered saline (pH 7.4), blotted dry, and weighed. The schematic presentation of the experimental design is depicted in Suppl. Fig. 1.

Evaluation of Biochemical Parameters

Evaluation of Plasma Parameters

The aspartate aminotransferase (SGOT/AST; IFCC method), alanine aminotransferase (SGPT/ALT; IFCC method), bilirubin total (BiT; Diazo method, endpoint), and γ-glutamyl transferase (GLUPA, γ-GT; IFCC method) were evaluated in liver or plasma using reagents and semi auto-analyzer provided by ERBA Diagnostics, Mannheim, Germany.

Evaluation of Triglycerides, Hydroxyproline, and NLRP3 in Liver

Rat NLRP3 ELISA (E-EL-R1463) and hydroxyproline colorimetric assay kits (E-BC-K062-S) were purchased from Elabscience, TX, USA. Triglycerides (GPO-Trinder method) level was measured provided by ERBA Diagnostics, Mannheim, Germany. The total protein levels were estimated by mixing supernatant with solution D containing 2% Na_2CO_3, 0.4% NaOH, 0.04% $KNaC_4H_4O_6{\cdot}4H_2O$, and 0.02% $CuSO_4$ for 10 min at 37 °C. The resultant solution was further mixed with an equal volume of Folin-Ciocalteu reagent at 37 °C for 30 min [25].

Evaluation of Cellular Damage

Liver sections were processed for the staining procedure of deparaffinization, dehydration, and staining with hematoxylin & eosin (H&E), dehydration, and DPX mounting. Picro-sirius red and Masson's trichrome stains were performed to evaluate collagen deposition, as described previously [26]. The necro-inflammatory scoring with H&E staining and staging of liver fibrosis with picro-sirius red staining were adapted from a modified Ishak system (Suppl. Tables 1 and 2) [27, 28]. For the histological observation and analyses, at least 20 images/focuses (at a total magnification of 400×) were taken randomly from each sample, and percent fibrotic areas were quantified using the ImageJ software (version 1.44p, NIH, Bethesda, USA).

Evaluation of Immunohistochemical/Immunofluorescence Analyses

Liver sections were deparaffinized using xylene, hydrated in gradients of alcohol, and processed further for immunohistochemical/immunofluorescence analysis by using either ImmPRESS excel staining kit (Vector lab, CA, USA) as per the protocol suggested by the manufacturer. Primary rabbit/mouse/goat polyclonal/monoclonal antibodies of NLRP3 (sc-66846), 8-OHdG (sc-66036) caspase p10 (sc-514), ASC (N-15)-R (sc-22514), TGF-β1 (sc-146), and IL-1β (sc-7884) were diluted (1:50) and incubated overnight at 4 °C as described previously [29]. Subsequently, liver sections were incubated with amplifier antibodies and FITC- or HRP-conjugated secondary antibodies. Finally, sections were further incubated with 3,3′-diaminobenzidine at 37 °C for 10–20 min, stained with hematoxylin, dehydrated, and mounted. For the IHC analyses, at least 20 images/focuses (at a total magnification of 400×) were taken from each sample, and percent immunopositive areas were quantified using the ImageJ software (version 1.44p, NIH, Bethesda, USA).

Evaluation of Proteins Expressions by Western Blot

Approximately 100–150 mg of liver tissue was homogenized in RIPA buffer containing protease inhibitors, centrifuged as 10,000×*g* for 10 min, and supernatants were collected. Total protein level was determined, and protein concentration was kept constant at 3 mg/ml. Supernatants were mixed with sample buffers and were separated on 8–15% sodium dodecyl sulfate–polyacrylamide gel electrophoresis as described elsewhere [30]. Primary monoclonal or polyclonal antibodies of catalase (sc-50,508), pro caspase-1 + p10 + p12 (ab-179,515), SOD-1 (sc-11407), Nrf2 (sc-722), IL-6 (sc-1265), NF-κB p50 (sc-114), and β-actin (sc47778 HRP) from mouse or goat or rabbit (in

1:250–1500 dilution in TBS) incubated with membrane overnight at 4 °C. After washing, the membrane was incubated with HRP-conjugated secondary antibodies against primary antibodies (Promega Corporation, WI, USA, or Santa Cruz, CA, USA). Detection was done using western blotting luminol reagent (sc-2048, Santa Cruz, CA, USA) and X-ray films. The optical density analyses of band intensity on X-ray films were done by ImageJ (1.44p, NIH, Bethesda, USA).

Statistical Analyses

Data sets were processed for statistical analyses using GraphPad prism 6 (Statistical Software, California corporation, USA). For multiple comparisons, a one-way analysis of variance (ANOVA) followed by post hoc analysis with Tukey's test was performed. The level of significance was indicated by asterisks (*) as below, if $p < 0.05$ then indicated as *, if $p < 0.01$ then indicated as **, and if $p < 0.001$ then indicated as ***. All the results were expressed as mean ± standard deviation (SD).

RESULTS

Intervention with GLB, DMF, MCC950, 4OI, and Their Selected Combinations Reduced TAA-Induced Hepatic Damage

Morphological analyses at the time of necropsy from the TAA-exposed group showed a diffused fibrosis with mild discoloration of the liver compared with control, whereas such morphological changes were mildly attenuated with interventions of GLB, DMF, GLB + DMF, MCC950, 4OI, and MCC + 4OI compared with TAA control (Suppl. Fig. 2). TAA treatment significantly decreased body weight ($p < 0.01$) and increased the liver weight ($p < 0.001$) and liver coefficient [(liver to

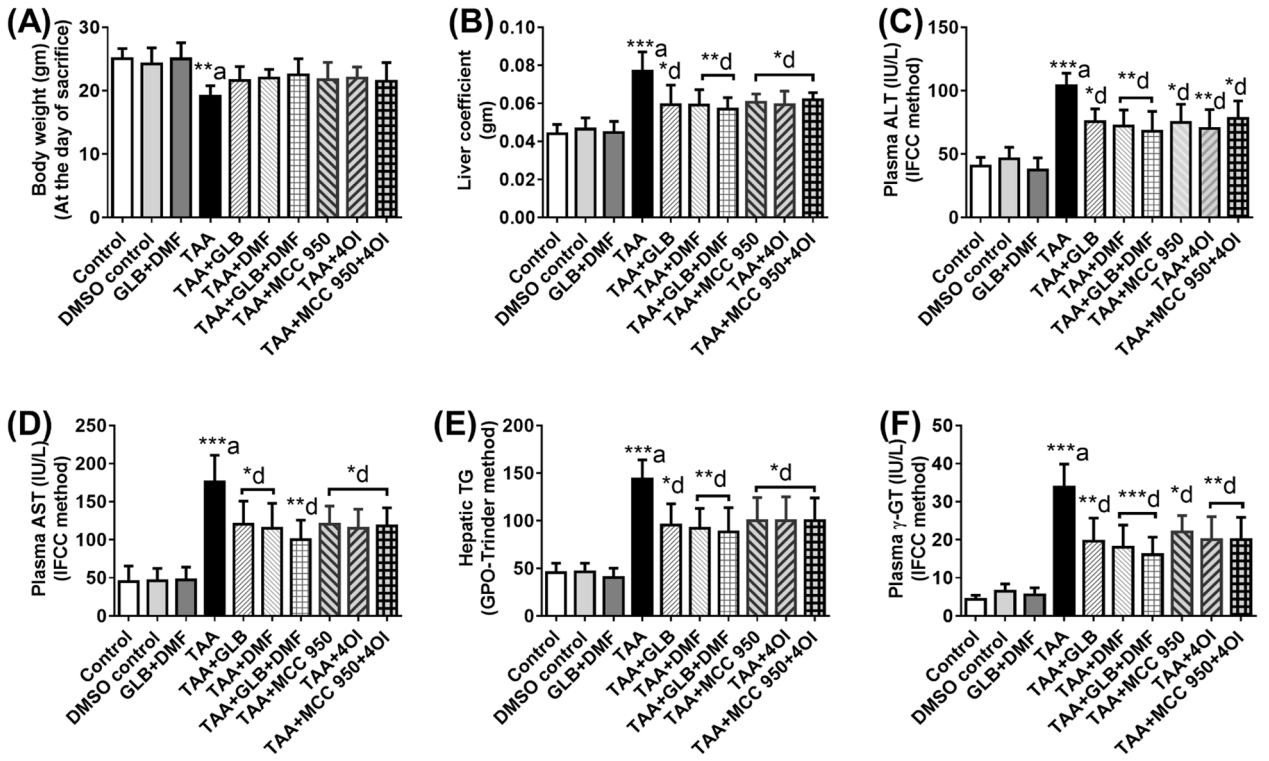

Fig. 1 The effect of GLB, DMF, GLB + DMF, MCC950, 4OI, and MCC950 + 4OI treatment on **A** body weight (at the day of sacrifice), **B** liver coefficient (liver to body weight ratio), **C** plasma alanine aminotransferase (ALT), **D** plasma aspartate aminotransaminase (AST), **E** hepatic triglycerides (TG), and **F** γ-glutamyl transferase (γ-GT) levels altered by TAA. Values are expressed as mean ± SD ($n = 5$ for each group), *$p < .05$, **$p < .01$, and ***$p < .001$, "a" vs control, "d" vs TAA.

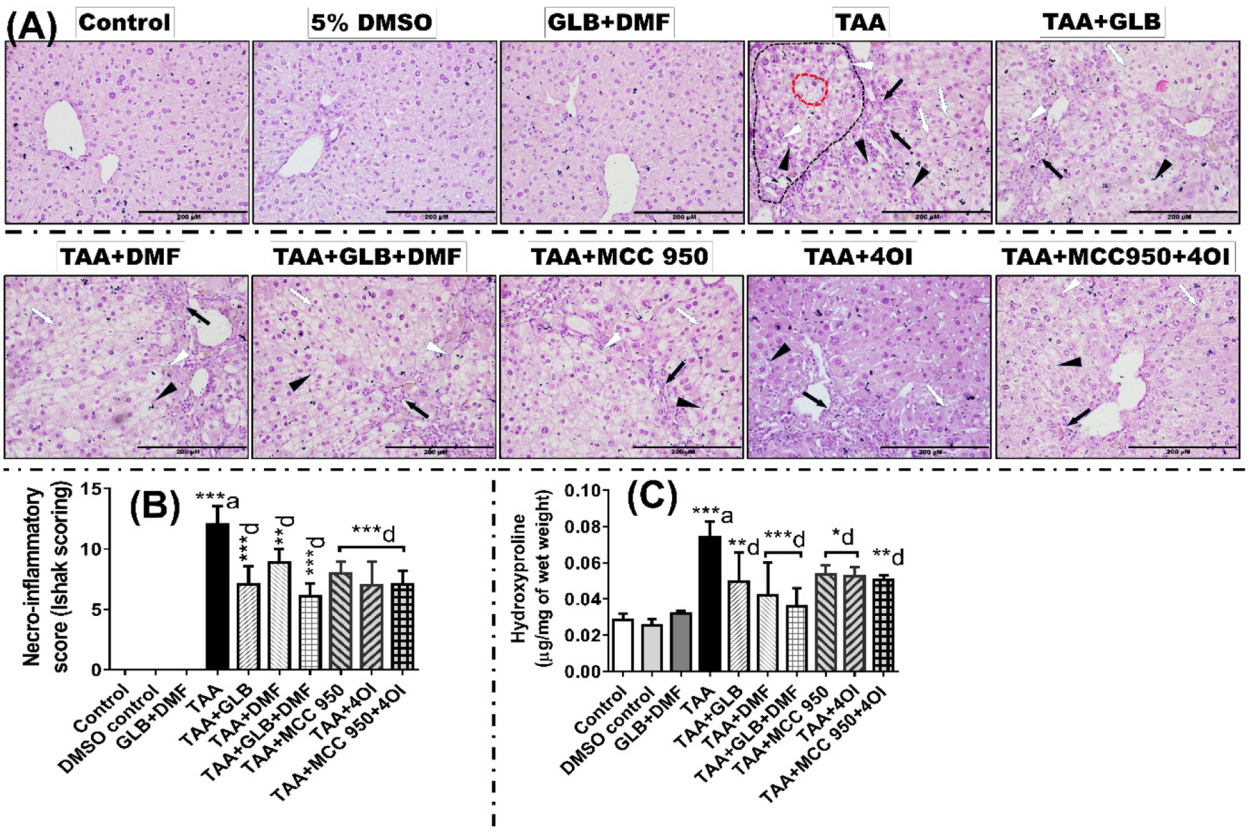

Fig. 2 **A** Representative photomicrographs with quantification from different groups showing H&E staining, **B** necro-inflammatory scoring, and **C** hydroxyproline content. The TAA-exposed group was observed with an area of hepatocellular damage surrounded by inflammatory cell infiltration (marked with black dashed lines), single enlarged hepatocyte (marked with red dashed lines), hepatocyte enlargement with large vacuolization (white arrowhead), macrovascular steatosis (black arrowhead), microvascular steatosis (white arrow), and inflammatory cell infiltrations (black arrow). Values are expressed as mean ± SD ($n = 3$), *$p < 0.05$, **$p < 0.01$, and ***$p < 0.001$, "a" vs control, "d" vs TAA.

body weight ratio), ($p < 0.001$)] compared with control. Interventions with GLB, DMF, GLB + DMF, MCC950, 4OI, and MCC950 + 4OI did not significantly increase body weight and decrease liver weight compared with TAA control (Fig. 1A; Suppl. Fig. 3A). Intervention with GLB ($p < 0.05$), DMF ($p < 0.01$), GLB + DMF ($p < 0.01$), MCC950 ($p < 0.05$), 4OI ($p < 0.05$), and MCC950 + 4OI ($p < 0.05$) significantly decreased liver coefficient compared with TAA control (Fig. 1B). TAA treatment significantly increased ($p < 0.001$) the plasma levels of ALT, AST, γ-GT, total bilirubin, and hepatic triglycerides (TG) compared with control. Interventions with GLB ($p < 0.05$), DMF ($p < 0.01$), GLB + DMF ($p < 0.01$), MCC950 ($p < 0.05$), 4OI ($p < 0.01$), and MCC950 + 4OI ($p < 0.05$) significantly decreased plasma ALT compared with TAA control (Fig. 1C). Interventions with GLB ($p < 0.05$), DMF ($p < 0.05$), GLB + DMF ($p < 0.01$), MCC950 ($p < 0.05$), 4OI ($p < 0.05$), and MCC950 + 4OI ($p < 0.05$) significantly decreased plasma AST compared with TAA control (Fig. 1D). Interventions with GLB ($p < 0.05$), DMF ($p < 0.01$), GLB + DMF ($p < 0.01$), MCC950 ($p < 0.05$), 4OI ($p < 0.05$), and MCC950 + 4OI ($p < 0.05$) significantly decreased hepatic TG compared with TAA control (Fig. 1E). Interventions with GLB ($p < 0.01$), DMF ($p < 0.001$), GLB + DMF ($p < 0.001$), MCC950 ($p < 0.05$), 4OI ($p < 0.01$), and MCC950 + 4OI ($p < 0.01$) significantly decreased plasma γ-GT compared with TAA control (Fig. 1F). Interventions with GLB ($p < 0.05$), DMF ($p < 0.001$), GLB + DMF ($p < 0.001$), MCC950 ($p < 0.01$), 4OI ($p < 0.01$), and MCC950 + 4OI ($p < 0.001$) significantly decreased plasma bilirubin compared with TAA control (Suppl Fig. 3B).

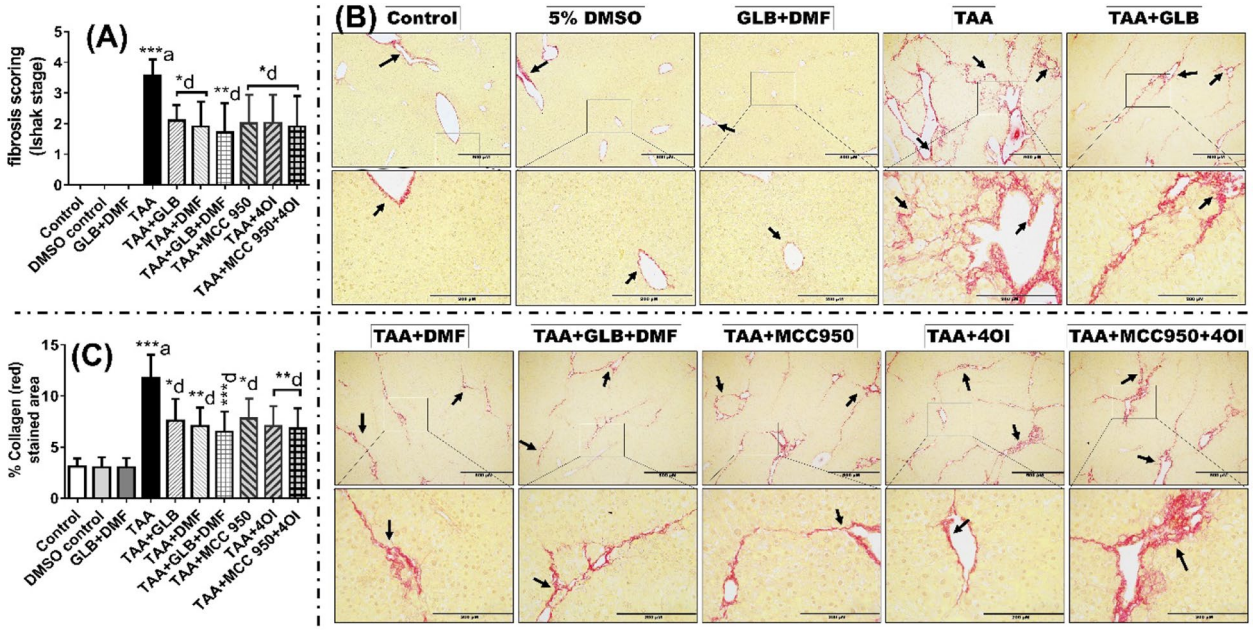

Fig. 3 The effect of GLB, DMF, GLB + DMF, MCC950, 4OI, and MCC950 + 4OI treatment on **A** fibrosis scoring and **B** representative photomicrographs with quantification showing picro-sirius red staining and **C** quantification of percent fibrotic area in liver. The TAA treatment revealed the deposition of collagen (indicated by the black arrow, collagen has stained red against a yellow background), which expands in the form of fibrous septae, divided liver into pseudolobules (indicated by an asterisk), and termed as bridging fibrosis. Values are expressed as mean ± SD ($n = 3$), *$p < 0.05$, **$p < 0.01$, and ***$p < 0.001$, "a" vs control, "d" vs TAA.

Intervention with GLB, DMF, MCC950, 4OI, and Their Selected Combinations Decreased the Development of TAA-Induced Fibrosis

Histopathological analyses revealed inflammatory cell infiltration, necrosis, macrovascular, and microvascular steatosis in the TAA-exposed group compared with the control (Fig. 2A). Histopathological necro-inflammatory scoring, fibrosis scoring, and liver hydroxyproline were significantly increased ($p < 0.001$) in the TAA-exposed group compared with the control (Fig. 2B & C; 3A). The interventions with GLB ($p < 0.001$), DMF ($p < 0.01$), GLB + DMF ($p < 0.001$), MCC950 ($p < 0.001$), 4OI ($p < 0.001$), and MCC950 + 4OI ($p < 0.001$) significantly decreased necro-inflammatory score compared with TAA control (Fig. 2B). The interventions with GLB ($p < 0.01$), DMF ($p < 0.001$), GLB + DMF ($p < 0.001$), MCC950 ($p < 0.05$), 4OI ($p < 0.05$), and MCC950 + 4OI ($p < 0.01$) significantly decreased hydroxyproline compared with TAA control (Fig. 2C). The interventions with GLB ($p < 0.05$), DMF ($p < 0.05$), GLB + DMF ($p < 0.01$), MCC950 ($p < 0.05$), 4OI ($p < 0.05$), and MCC950 + 4OI ($p < 0.05$) significantly decreased fibrosis score compared with TAA control (Fig. 3A). Further, a hallmark of liver fibrosis was evident by picro-sirius red and Masson's trichrome staining, which revealed a significant increase ($p < 0.001$) in the collagen content in the TAA-exposed group compared with control. The interventions with GLB ($p < 0.05$), DMF ($p < 0.01$), GLB + DMF ($p < 0.001$), MCC950 ($p < 0.05$), 4OI ($p < 0.01$), and MCC950 + 4OI ($p < 0.01$) significantly decreased collagen compared with TAA control in picro-sirius red staining (Fig. 3B & C). The interventions with GLB ($p < 0.01$), DMF ($p < 0.01$), GLB + DMF ($p < 0.001$), MCC950 ($p < 0.05$), 4OI ($p < 0.01$), and MCC950 + 4OI ($p < 0.001$) significantly decreased collagen compared with TAA control in Masson's trichrome staining (Suppl. Fig. 4). Further, the immunoexpression analyses revealed a significant increase ($p < 0.001$) in the expressions fibrosis markers TGF-β1 and CTGF in the TAA group compared with control. The interventions with GLB ($p < 0.01$), DMF ($p < 0.001$), GLB + DMF ($p < 0.001$),

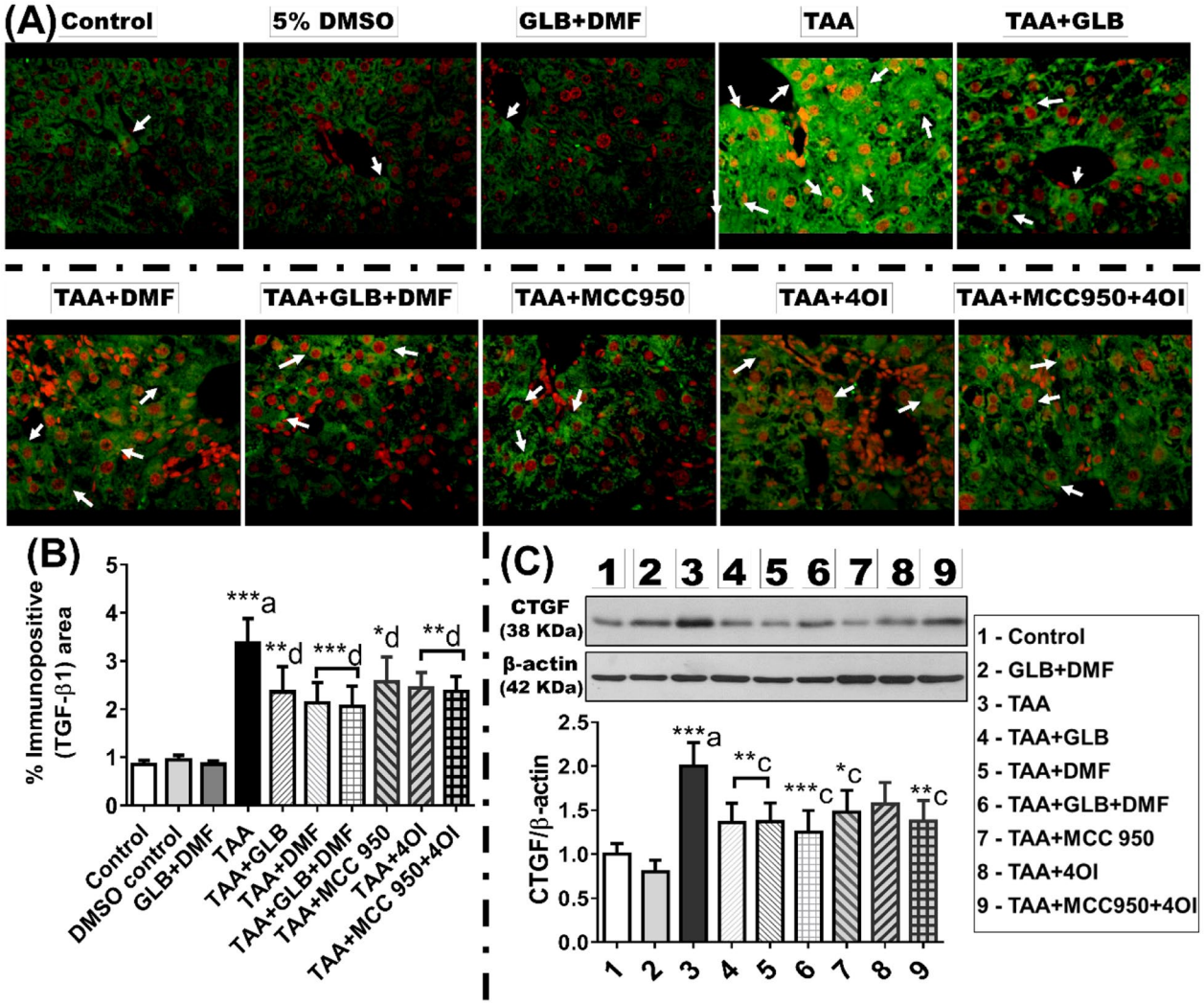

Fig. 4 **A** Representative photomicrographs with quantification from different groups showing TGF-β1 immunoexpression in the liver. White arrows indicate the immunopositive area (green against a black background) and **B** the effect of GLB, DMF, GLB + DMF, MCC950, 4OI, and MCC950 + 4OI treatment on CTGF expression. Values are expressed as mean ± SD ($n = 3$), *$p < 0.05$, **$p < 0.01$, and ***$p < 0.001$, "a" vs control, "d" vs TAA. The depiction of the vehicle control (5% DMSO) group has not been evaluated in the above protein expression profiles because no significant changes were observed compared with the control group in the biochemical and histological parameters. The same β-actin has been presented in Fig. 4B (CTGF/β-actin) and Fig. 8C (NF-κB/β-actin).

MCC950 ($p < 0.05$), 4OI ($p < 0.01$), and MCC950 + 4OI ($p < 0.01$) significantly decreased TGF-β1 compared with TAA control (Fig. 4A & B). The interventions with GLB ($p < 0.01$), DMF ($p < 0.01$), GLB + DMF ($p < 0.001$), MCC950 ($p < 0.05$), 4OI (no significance), and MCC950 + 4OI ($p < 0.01$) significantly decreased CTGF compared with TAA control (Fig. 4C).

Intervention with GLB, DMF, MCC950, 4OI, and Their Selected Combinations Reduced TAA-Induced Oxidative Stress

An oxidative stress in TAA-exposed animal was evident by a significant decrease ($p < 0.001$) in the expressions of Nrf2, HO-1, NQO-1, SOD-1, and catalase

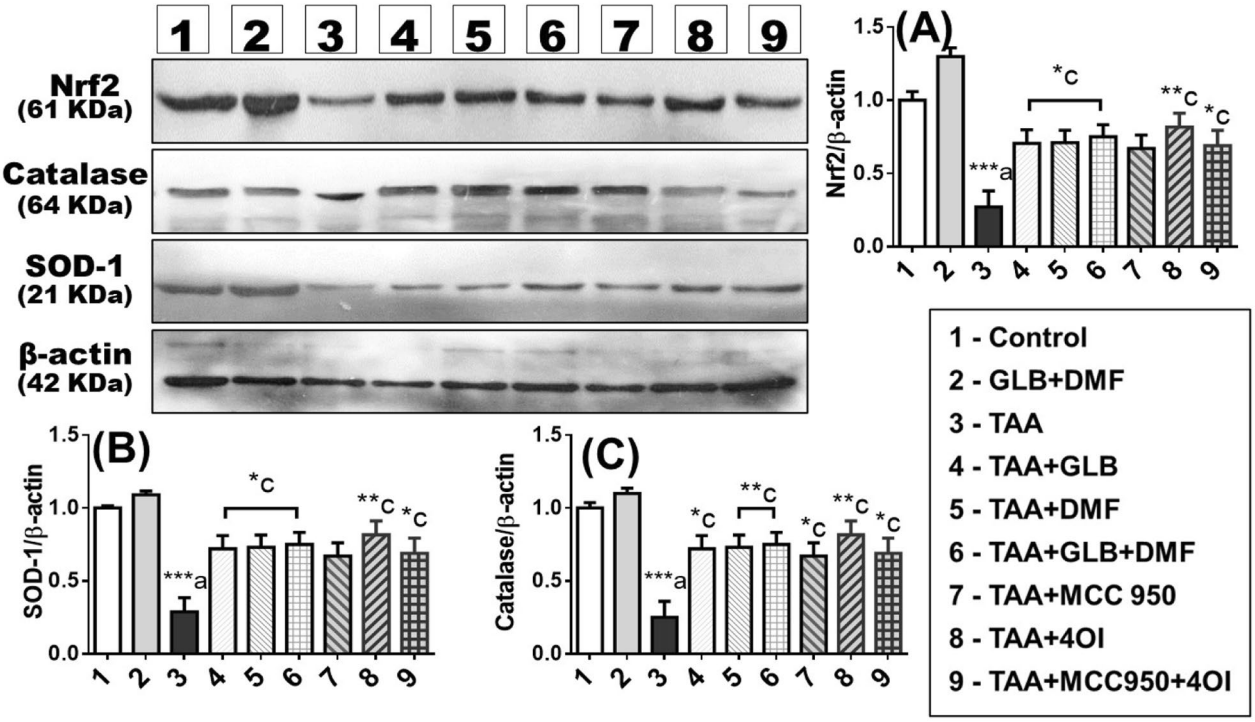

Fig. 5 Representative immunoblots with quantification from different groups showing **A** Nrf2, **B** SOD-1, and **C** catalase expressions in the liver. Values are expressed as mean ± SD ($n = 3$), *$p < 0.05$, **$p < 0.01$, and ***$p < 0.001$, "a" vs control, "c" vs TAA. The depiction of the vehicle control (5% DMSO) group has not been evaluated in the above protein expression profiles because no significant changes were observed compared with the control group in the biochemical and histological parameters.

as observed in immunoblot and immunofluorescence analyses and compared with the control. The interventions with GLB ($p < 0.05$), DMF ($p < 0.05$), GLB + DMF ($p < 0.05$), MCC950 (no significance), 4OI ($p < 0.01$), and MCC950 + 4OI ($p < 0.05$) significantly decreased Nrf2 and SOD-1 expressions compared with TAA control (Fig. 5A & B). The interventions with GLB ($p < 0.05$), DMF ($p < 0.01$), GLB + DMF ($p < 0.01$), MCC950 ($p < 0.05$), 4OI ($p < 0.01$), and MCC950 + 4OI ($p < 0.05$) significantly decreased catalase expression compared with TAA control (Fig. 5C). The interventions with GLB ($p < 0.05$), DMF ($p < 0.05$), GLB + DMF ($p < 0.01$), MCC950 ($p < 0.05$), 4OI ($p < 0.01$), and MCC950 + 4OI ($p < 0.01$) significantly decreased HO-1 expression compared with TAA control (Fig. 6). The interventions with GLB ($p < 0.05$), DMF ($p < 0.01$), GLB + DMF ($p < 0.001$), MCC950 ($p < 0.01$), 4OI ($p < 0.01$), and MCC950 + 4OI ($p < 0.001$) significantly decreased NQO-1 expression compared with TAA control (Suppl. Fig. 5).

Intervention with GLB, DMF, MCC950, 4OI, and Their Selected Combinations Decreased TAA-Induced NLRP3 Inflammasome Activation

The level of NLRP3 inflammasome was significantly increased in the TAA ($p < 0.001$) treated group, as evident by the NLRP3 ELISA test (Fig. 7A). Further, the involvement of NLRP3 inflammasome pathway in liver fibrosis was confirmed by the immunohistochemical analyses, which showed the increased expressions of NLRP3 ($p < 0.001$), ASC ($p < 0.001$), caspase-1 ($p < 0.001$), and IL-1β ($p < 0.001$) in TAA group compared with control (Fig. 7B & C, Suppl. Figs. 6-8). Furthermore, the activation of NLRP3 inflammasome was confirmed by the immunoblot analyses, which revealed an enhanced expression of active caspase-1 p10 (a sharp band at molecular weight 10 KDa) in the TAA group compared with control (Fig. 8A). The active caspase-1 is considered a hallmark for the activation of NLRP3

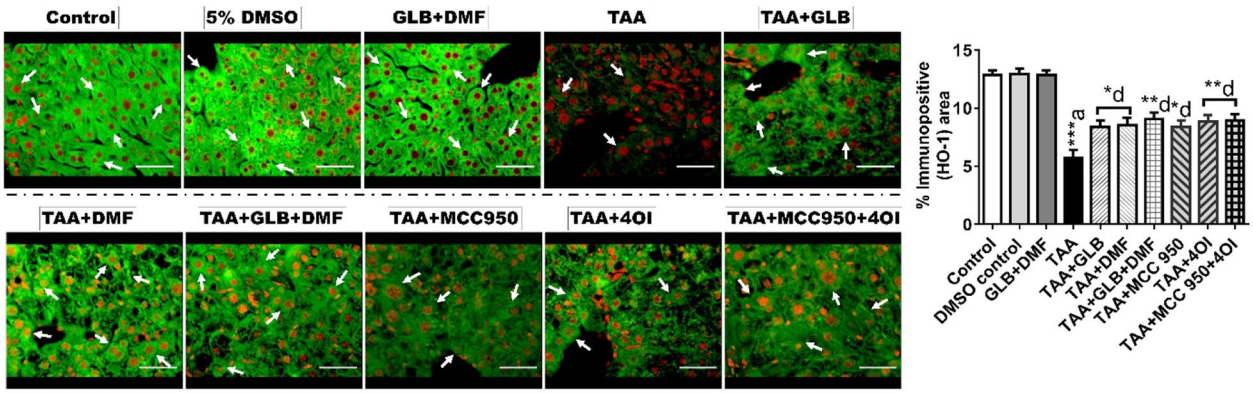

Fig. 6 Representative photomicrographs with quantification from different groups showing HO-1 immunoexpression in the liver. White arrows indicated the immunopositive area (green against a black background). Values are expressed as mean ± SD ($n = 3$), *$p < 0.05$, **$p < 0.01$, and ***$p < 0.001$, "a" vs control, "d" vs TAA.

inflammasome. The interventions with GLB ($p < 0.01$), DMF ($p < 0.001$), GLB + DMF ($p < 0.001$), MCC950 ($p < 0.001$), 4OI ($p < 0.05$), and MCC950 + 4OI ($p < 0.05$) significantly decreased NLRP3 level compared with TAA control during ELISA test analysis (Fig. 7A). The interventions with GLB ($p < 0.01$), DMF ($p < 0.01$), GLB + DMF ($p < 0.001$), MCC950 ($p < 0.001$), 4OI ($p < 0.05$), and MCC950 + 4OI ($p < 0.01$) significantly decreased NLRP3 immunoexpression compared with TAA control (Suppl. Fig. 6). Moreover, the interventions with GLB ($p < 0.01$), DMF ($p < 0.05$), GLB + DMF ($p < 0.01$), MCC950

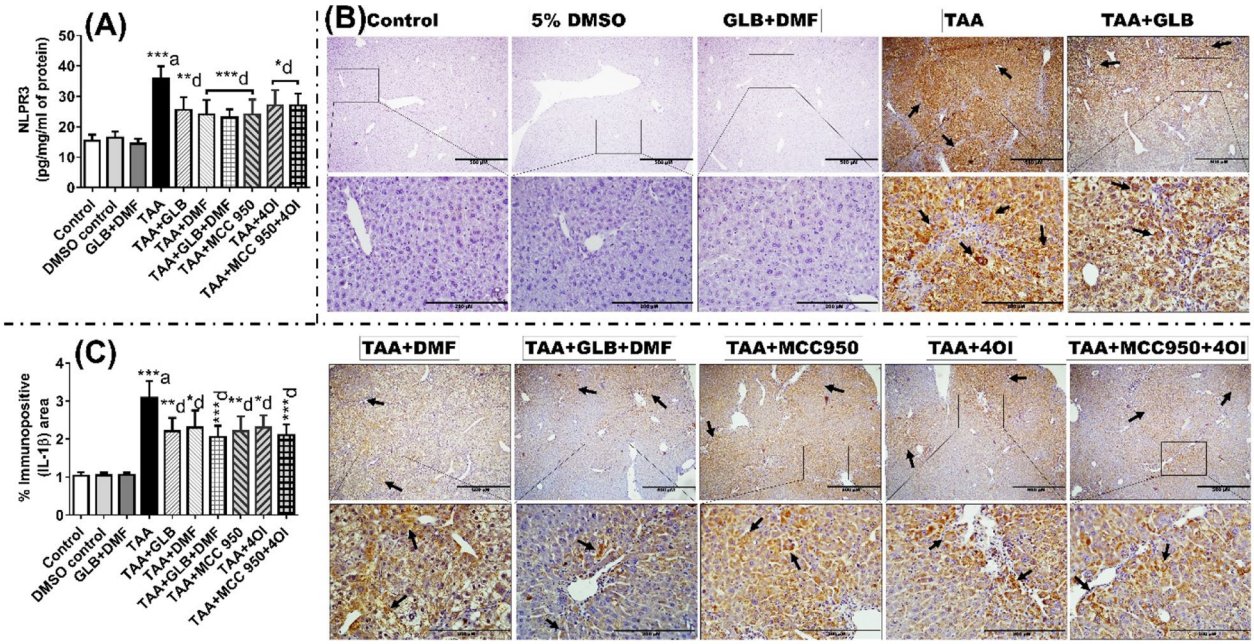

Fig. 7 **A** Representative photomicrographs with quantification from different groups showing IL-1β immunostaining in the liver. Black arrows indicated the immunopositive area, **B** the effect of GLB, DMF, GLB + DMF, MCC950, 4OI, and MCC950 + 4OI on NLRP3 level in TAA-induced hepatic damage. Values are expressed as mean ± SD ($n = 3$), *$p < 0.05$, **$p < 0.01$, and ***$p < 0.001$, "a" vs control, "d" vs TAA.

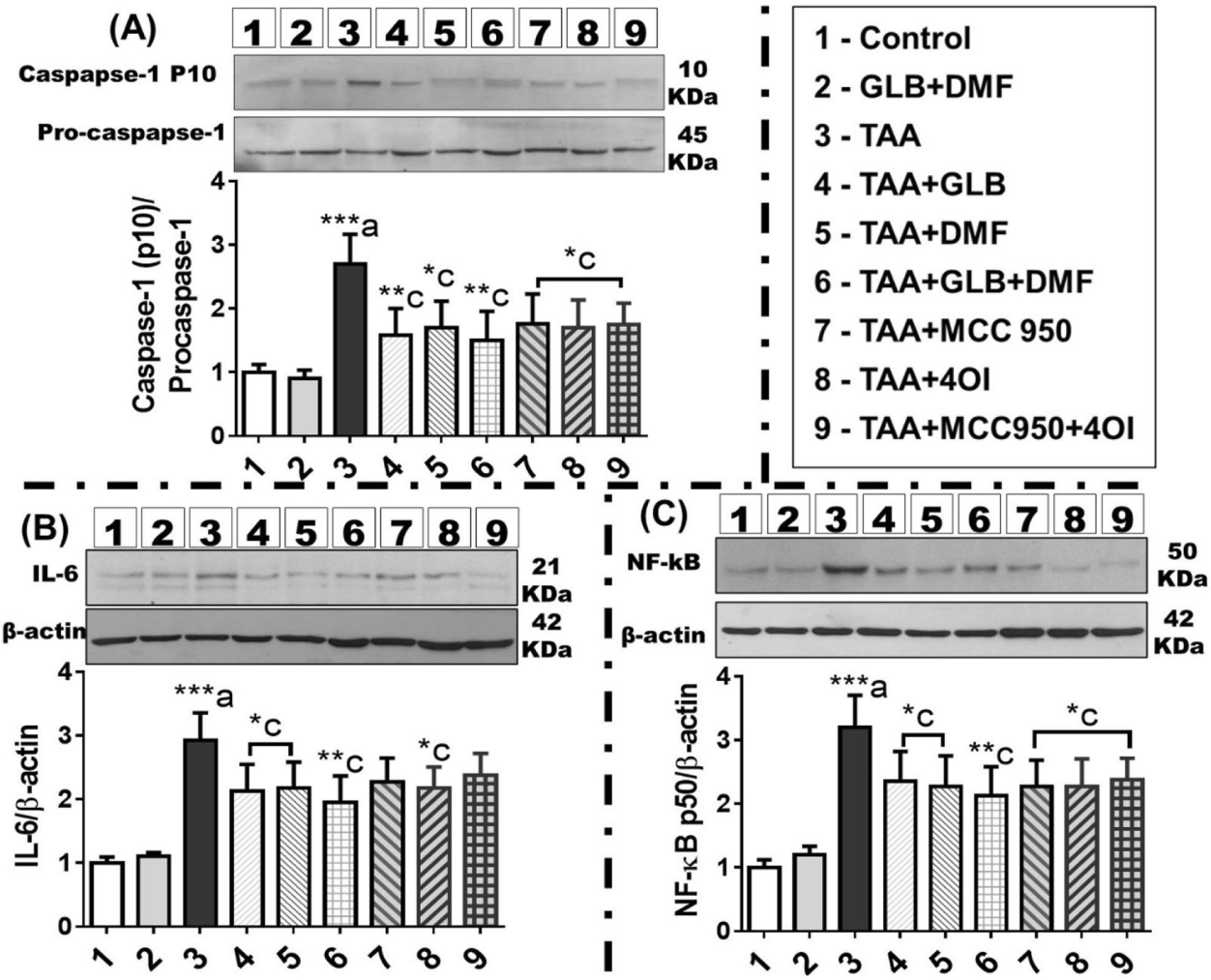

Fig. 8 Representative immunoblots with quantification from different groups showing **A** caspase-1 (p10)/pro-caspase-1 ratio, **B** IL-6, and **C** NF-κB expressions in the liver. Values are expressed as mean ± SD ($n = 3$), *$p < 0.05$, **$p < 0.01$, and ***$p < 0.001$, "a" vs control, "c" vs TAA. The depiction of the vehicle control (5% DMSO) group has not been evaluated in the above protein expression profiles because no significant changes were observed compared with the control group in the biochemical and histological parameters. The same β-actin has been presented in Fig. 4B (CTGF/β-actin) and Fig. 8C (NF-κB/β-actin).

($p < 0.01$), 4OI ($p < 0.05$), and MCC950 + 4OI ($p < 0.05$) significantly decreased ASC immunoexpression compared with TAA control (Suppl. Fig. 7). Further, the interventions with GLB ($p < 0.01$), DMF ($p < 0.05$), GLB + DMF ($p < 0.001$), MCC950 ($p < 0.01$), 4OI ($p < 0.05$), and MCC950 + 4OI ($p < 0.01$) significantly decreased caspase-1 p10 immunoexpression compared with TAA control (Suppl. Fig. 8). The interventions with GLB ($p < 0.01$), DMF ($p < 0.05$), GLB + DMF ($p < 0.001$), MCC950 ($p < 0.001$), 4OI ($p < 0.05$), and MCC950 + 4OI ($p < 0.001$) significantly decreased IL-1β immunoexpression compared with TAA control (Fig. 7B & C). Furthermore, the interventions with GLB ($p < 0.01$), DMF ($p < 0.05$), GLB + DMF ($p < 0.01$), MCC950 ($p < 0.05$), 4OI ($p < 0.05$), and MCC950 + 4OI ($p < 0.05$) significantly decreased caspase-1 p10 immunoexpression (immunoblot at 10 KDa) compared with TAA control (Fig. 8A).

Intervention with GLB, DMF, MCC950, 4OI, and Their Selected Combinations Reduced TAA-Induced Inflammation, DNA Damage, and Apoptosis

There was a significantly increase in the expressions of inflammatory markers IL-6 ($p < 0.001$) and NF-κB p50 ($p < 0.001$), DNA damage marker 8-OHdG ($p < 0.001$) and apoptosis marker caspase-3 ($p < 0.001$) were in TAA-treated group compared with control (Fig. 8B and C, Suppl. Figs. 9, 10). The interventions with GLB ($p < 0.05$), DMF ($p < 0.05$), GLB + DMF ($p < 0.01$), MCC950 (no significance), 4OI ($p < 0.05$), and MCC950 + 4OI (no significance) significantly decreased hepatic IL-6 immunoexpression compared with TAA control (Fig. 8B). The interventions with GLB ($p < 0.05$), DMF ($p < 0.05$), GLB + DMF ($p < 0.01$), MCC950 ($p < 0.05$), 4OI ($p < 0.05$), and MCC950 + 4OI ($p < 0.05$) significantly decreased hepatic NF-κB p50 immunoexpression compared with TAA control (Fig. 8C). The interventions with GLB ($p < 0.01$), DMF ($p < 0.01$), GLB + DMF ($p < 0.001$), MCC950 ($p < 0.05$), 4OI ($p < 0.05$), and MCC950 + 4OI ($p < 0.05$) significantly decreased hepatic 8-OHdG immunoexpression compared with TAA control (Suppl. Fig. 9). The interventions with GLB ($p < 0.05$), DMF ($p < 0.01$), GLB + DMF ($p < 0.001$), MCC950 ($p < 0.05$), 4OI ($p < 0.01$), and MCC950 + 4OI ($p < 0.01$) significantly decreased hepatic caspase-3 immunoexpression compared with TAA control (Suppl. Fig. 10).

DISCUSSION

Liver fibrosis is the formation of scars upon repetitive liver injury that impairs normal liver functioning. Persistent liver fibrosis results in an end-stage liver disease named cirrhosis, which treatment mostly needs liver transplantation from a healthy liver donor. Exposure to TAA significantly induced mild liver discoloration, decreased body weight, increased liver weight, and liver to body weight ratio compared with control. TAA exposure led to a significant increase in the plasma levels of ALT, AST, γ-GT, total bilirubin, and hepatic levels of triglycerides, hydroxyproline, and NLRP3 compared with control, while treatment with GLB, DMF, GLB + DMF, MCC950, 4OI, and MC950 + 4OI significantly decreased these parameters. TAA induced significant increase in the liver weight and liver index, which was due to the deposition of collagen, induction of angiogenesis process, and increased fibrotic components. An increase in liver function test parameters in TAA-exposed mice was due to the damage to the hepatocytes. Chen et al. reported that a combination of GLB with AC-YVAD-CMK decreased cecal ligation and puncture (CLP)-induced acute liver injury in mice by decreasing inflammatory infiltrations, pyroptosis, serum concentrations of ALT, AST, IL-1β, IL-18, and liver expressions of caspase-1 [31]. It has been reported that treatment with DMF decreased the liver to body weight ratio in acetaminophen-induced liver injury in mice [32]. Wang et al. reported that intraperitoneal treatment with MCC950 at 3 mg/kg for 7 days attenuates D-galactosamine-induced acute liver failure in mice by decreasing the serum ALT, AST activity, and hepatic expressions of IL-1β and IL-18 [33]. Intraperitoneal intervention with 4OI at 25 mg/kg before 2 h of ischemia–reperfusion (I/R) protects hepatocytes from I/R-induced hypoxia by activating the Nrf2 pathway and by decreasing ALT activity, necrosis, and LDH release in mice [23].

Exposure of TAA results in apoptosis as revealed by increased capspae-3 expression and in DNA damage as indicated by increased 8-OHdG expression. Intervention with GLB, DMF, GLB + DMF, MCC950, 4OI, and MC950 + 4OI reduced DNA damage and apoptosis. Further, histological findings showed the increase in inflammatory infiltrations, necro-inflammatory score, ballooned hepatocytes, bridging fibrosis, and centrilobular necrosis in the livers of TAA-exposed mice. The establishment of liver fibrosis was confirmed by an increase in the Ishak scoring system in the liver of TAA-exposed mice. Furthermore, picro-sirius red and Masson's trichrome staining revealed the collagen deposition in the portal and central vein areas in the liver of TAA-exposed mice. The decrease in collagen level was further evident by the decreased level of hydroxyproline content in the TAA-exposed liver. Further, TAA exposure also increased the expressions of several fibrogenic as well as fibrosis markers such as TGF-β1 and CTGF. Intervention with GLB, DMF, GLB + DMF, MCC950, 4OI, and MC950 + 4OI significantly decreased the several histological alterations, Ishak fibrosis scoring, necro-inflammatory scoring, collagen deposition, hydroxyproline content, and immunoexpressions of fibrogenic and fibrosis markers. De David et al. reported that TAA exerts a hepatotoxic effect by producing ROS and free radicals and damages different components of the cell, including proteins,

lipids, and DNA in Wistar rats [34]. Treatment with GLB has been reported to reduced intranucleosomal DNA fragmentation, thereby decreased DNA damage in the liver of type I diabetic rats [35]. Schupp et al. reported that DMF treatment reduced carboxy(methyl)lysine-modified BSA-induced percent DNA in the proximal tubular cells (LLC-PK1) of the pig [36]. Intraperitoneal intervention with MCC950 at the dosage of 2.5 and 5 mg/kg once a day for 2 weeks has been reported to ameliorate liver fibrosis by inhibiting the NLRP3 inflammasome activation and by downregulating expressions of IL-1β, α-SMA, col1α1, and TGF-β in CCl_4-induced liver injury in mice [37]. Intravenous treatment with 4-OI at 1 and 10 mg/kg for 3 weeks has been reported to protect adenine-induced renal fibrosis in the Sprague–Dawley rats model by suppressing ROS production, inhibiting autophagy, and by downregulating TGF-β/Smad and NF-κB signaling [24].

A significant increase in oxidative stress as evidenced by decreased expressions of Nrf-2, HO-1, NQO-1, SOD-1, and catalase in TAA-exposed livers. Chronic exposure of TAA significantly increased inflammation as indicated by enhanced expressions pro-inflammatory transcription factor NF-κB, IL-6, NLRP3 inflammasome, its adapter protein ASC, active product caspase-1, and downstream product IL-1β. The activation of NLRP3 inflammasome was further confirmed by the immunoblot analysis of caspase-1, in which the functional form caspase-1 p10 at molecular weight 10 KDa was observed. The antioxidant and anti-inflammatory activity of GLB, DMF, GLB + DMF, MCC950, 4OI, and MCC950 + 4OI was confirmed by the restoration of TAA-induced changes in oxidative stress and inflammation; hence, these interventions reduced the oxidative stress and inflammation associated with the progression of liver fibrosis. Wree et al. reported that NLRP3 activation results in hepatocyte pyroptosis, liver inflammation, and subsequently fibrosis [38]. An interesting research by Watanabe et al. reported that NLRP3 and ASC knocked out mice, which did not develop hepatic fibrosis when injected with carbon tetrachloride and TAA [39]. It has already been reported that NF-κB signaling is essential for the proper activation of NLRP3 inflammasome in primary cultured hepatocytes [40]. Benitez et al. reported that GLB and a caspase-1 inhibitor Y-VAD-FMK reduced percent hepatic fibrotic area from *Brucella abortus*-infected NLRP3, ASC, AIM2, and caspase-1/11 knockout mice compared with *B. abortus*-infected wild-type mice [41]. An interesting report by Garstkiewicz et al. demonstrated that Nrf2 positively regulates NLRP3 inflammasome, but Nrf2-activator DMF inhibits inflammasome activation and concludes that these both stress-related pathways activated simultaneously upon stress signaling [42]. Treatment with DMF has been reported to prevent ATP-induced pyroptosis of THP-1 cells by decreasing caspase-1 and interleukin-1β release [43]. Moreover, Giustina and colleagues reported that DMF reduced oxidative stress and inflammation associated with CLP-induced sepsis in Wistar rats by increasing the SOD and catalase activities in the heart, liver, and lung [44]. Treatment with MCC950 has been reported to abrogate the palmitic acid-induced expressions of NLRP3, caspase-1, IL-1β, and IL-18, as well as activity of caspase-1 in primary hepatocytes from rats [45]. The intraperitoneal 4OI treatment at 50 mg/kg has been reported to exhibit an anti-inflammatory effect against LPS-induced lethal endotoxemia by decreasing the serum levels of IL-1β, IL-6, lactate, and IL-1β mRNA level in both RAW264.7 macrophages and BMDMs from mice [46].

The authors have previously reported that intervention with GLB and DMF significantly ameliorates TAA-induced alterations in plasma/serum levels of ALT, AST, ALP, γ-GT, bilirubin, uric acid, and hepatic MDA, ROS, SOD, collagen deposition, histological architecture, HSCs activation, apoptosis, DNA damage, TGF-β1, α-SMA, fibronectin, NLRP3, ASC, caspase-1, IL-1β, Nrf2, SOD-1, and catalase in Wistar rats [10, 47]. Further, the authors have also reported that intervention with GLB, DMF, and their combination GLB + DMF significantly ameliorated DEN + TAA-induced alterations in plasma levels of ALT, AST, ALP, uric acid, and hepatic triglycerides, apoptosis, histological architecture, and immunoexpression of NLRP3, ASC, caspase-1, IL-1β, Nrf2, HO-1, NQO-1, SOD-1, catalase, TGF-β1, collagen-1, 8-OHdG, GST-P, STAT3, AFP, PCNA, HGF, c-MET, TGFα, and EGF in partially hepatectomized Wistar rats [20].

On the basis of our present results and previously reported outcomes, it could be concluded that simultaneous and specific inhibition of NLRP3 inflammasome signaling by GLB and MCC950 and activation of Nrf2/ARE pathway by DMF and 4OI ameliorated TAA-induced hepatic fibrosis in rodents. As the authors have hypothesized that combination treatment with specific NLRP3 inhibitor MCC950 and Nrf2 activator 4OI could completely reverse/ameliorate liver fibrosis; however, there was no complete amelioration was observed with the combined treatment of the specific inhibitor/activator. Moreover, the present objective was aimed to compare the hepatoprotective effect of GLB versus

MCC950, DMF versus 4OI, and GLB + DMF versus MCC950 + 4OI; however, no significant comparison was observed when compared with alone or combination intervention. Treatment of GLB + DMF showed a higher level of significance compared with alone GLB and DMF treatment in approximately all of the parameters against TAA-induced hepatic damage. The GLB, DMF, and GLB + DMF intervention exhibited better protective effects compared with MCC950, 4OI, and MCC950 + 4OI, which revealed that this specific inhibitor/activator possesses only NLRP3 inflammasome inhibitory/Nrf2 activatory properties. In contrast, the clinical drug GLB and DMF possess some other beneficial effects, which are independent of NLRP3 inhibition or Nrf2 activation. Zhang et al. reported that, besides exhibiting insulin-releasing anti-diabetic effect, GLB also exerts anti-inflammatory effect in respiratory, digestive, urological, cardiological, ischemia–reperfusion injury, and CNS diseases by suppressing the production of ROS and proinflammatory mediators TNF-α and IL-1β, which indicate that the anti-inflammatory activity of GLB may occur through other/alternative pathways that are independent of NLRP3 inhibition [6]. Schulze-Topphoff et al. reported that DMF treatment provided equal protective effect in acute experimental autoimmune encephalomyelitis (EAE) in Nrf2-knockout and wild-type mice, which indicate that the anti-inflammatory activity of DMF may occur through alternative pathways that are independent of Nrf2 activation [48]. The overall finding of the present study indicated that simultaneously targeting NLRP3 inflammasome inhibition and Nrf2/ARE pathway activation could be one of the successful strategies to ameliorate oxidative stress- and inflammation-associated liver fibrosis.

SUPPLEMENTARY INFORMATION

The online version contains supplementary material available at https://doi.org/10.1007/s10753-021-01571-3.

ACKNOWLEDGEMENTS

The authors are thankful to the National Institute of Pharmaceutical Education and Research, SAS Nagar, India, for providing financial assistance to carry out the present experimentation. The authors are grateful to the anonymous reviewers for their critical suggestions to improve the quality and scientific clarity of the manuscript.

AUTHOR CONTRIBUTION

Durgesh K. Dwivedi conceived, conducted the experiments, analyzed the data, and wrote the manuscript. G. B. Jena conceived the idea, reviewed the manuscript, and administered the project. Finally, both the authors have read and approved the manuscript.

FUNDING

The authors are thankful to the National Institute of Pharmaceutical Education and Research, SAS Nagar, India, for providing financial assistance to carry out the present experimentation. Durgesh K. Dwivedi had presented this study at the virtual annual meeting of the Society of Toxicology, USA, on 17 March 2021.

AVAILABILITY OF DATA AND MATERIAL

All data and materials support their published claims and comply with field standards. Data will be available on demand.

CODE AVAILABILITY

It is not applicable in present research.

DECLARATIONS

Ethical Approval All institutional and national guidelines for the care and use of laboratory animals were followed. The animal studies were approved by the Ethics Committee of the NIPER SAS Nagar (IAEC/19/15).

Informed Consent Informed consent is not applicable in the present study.

Plant Reproducibility It is not applicable in present research.

Clinical Trials Registration It is not applicable in present research, as the experiments were performed in mice.

Consent to Participate It is not applicable in present research.

Consent for Publication Both authors are willing to publish their research work.

Conflict of Interest The authors declare no competing interests.

REFERENCES

1. Asrani, Sumeet K., Harshad Devarbhavi, John Eaton, and Patrick S. Kamath. 2019. Burden of liver diseases in the world. *Journal of hepatology* 70: 151–171. https://doi.org/10.1016/j.jhep.2018.09.014.
2. Sepanlou, Sadaf G., Saeid Safiri, Catherine Bisignano, Kevin S. Ikuta, Shahin Merat, Mehdi Saberifiroozi, Hossein Poustchi, et al. 2020. The global regional and national burden of cirrhosis by cause in 195 countries and territories 1990–2017: A systematic analysis for the Global Burden of Disease Study 2017. *The Lancet gastroenterology & hepatology* 5: 245–266. https://doi.org/10.1016/S2468-1253(19)30349-8.
3. Wallace, M.C., K. Hamesch, M. Lunova, Y. Kim, R. Weiskirchen, P. Strnad, and S.L. Friedman. 2015. Standard operating procedures in experimental liver research: Thioacetamide model in mice and rats. *Laboratory animals* 49: 21–29. https://doi.org/10.1177/0023677215573040.
4. Li, Sha, Hor-Yue. Tan, Ning Wang, Zhang-Jin. Zhang, Lixing Lao, Chi-Woon. Wong, and Yibin Feng. 2015. The role of oxidative stress and antioxidants in liver diseases. *International Journal of Molecular Sciences* 16: 26087–26124. https://doi.org/10.3390/ijms161125942.
5. Dixon, Laura J., Chris A. Flask, Bettina G. Papouchado, Ariel E. Feldstein, and Laura E. Nagy. 2013. Caspase-1 as a central regulator of high fat diet-induced non-alcoholic steatohepatitis. *PLoS ONE* 8: e56100. https://doi.org/10.1371/journal.pone.0056100.
6. Zhang, Gensheng, Xiuhui Lin, Shufang Zhang, Huiqing Xiu, Chuli Pan, and Wei Cui. 2017. A protective role of glibenclamide in inflammation-associated injury. *Mediators of inflammation* 2017: 3578702. https://doi.org/10.1155/2017/3578702.
7. Lamkanfi, Mohamed, James L. Mueller, Alberto C. Vitari, Shahram Misaghi, Anna Fedorova, Kurt Deshayes, Wyne P. Lee, Hal M. Hoffman, and Vishva M. Dixit. 2009. Glyburide inhibits the Cryopyrin/Nalp3 inflammasome. *The Journal of Cell Biology* 187: 61–70. https://doi.org/10.1083/jcb.200903124.
8. Koh, Gavin C K W., Tassili A. Weehuizen, Katrin Breitbach, Kathrin Krause, Hanna K. de Jong, Liesbeth M. Kager, Arjan J. Hoogendijk, et al. 2013. Glyburide reduces bacterial dissemination in a mouse model of melioidosis. *PLoS neglected tropical diseases* 7: e2500. https://doi.org/10.1371/journal.pntd.0002500.
9. Sharma, Ritu S., David J. Harrison, Dorothy Kisielewski, Diane M. Cassidy, Alison D. McNeilly, Jennifer R. Gallagher, Shaun V. Walsh, et al. 2018. Experimental nonalcoholic steatohepatitis and liver fibrosis are ameliorated by pharmacologic activation of Nrf2 (NF-E2 p45-related factor 2). *Cellular and molecular gastroenterology and hepatology* 5: 367–398. https://doi.org/10.1016/j.jcmgh.2017.11.016.
10. Dwivedi, D.K., Gopabandhu Jena, and Vinod Kumar. 2020. Dimethyl fumarate protects thioacetamide-induced liver damage in rats: Studies on Nrf2 NLRP3 and NF-κB. *Journal of biochemical and molecular toxicology* 34: e22476. https://doi.org/10.1002/jbt.22476.
11. Coll, Rebecca C., Avril A B. Robertson, Jae Jin Chae, Sarah C. Higgins, Raúl. Muñoz-Planillo, Marco C. Inserra, Irina Vetter, Lara S. Dungan, Brian G. Monks, and Andrea Stutz. 2015. A small-molecule inhibitor of the NLRP3 inflammasome for the treatment of inflammatory diseases. *Nature medicine* 21: 248.
12. Mridha, Auvro R., Alexander Wree, Avril A B. Robertson, Matthew M. Yeh, Casey D. Johnson, Derrick M. Van Rooyen, Fahrettin Haczeyni, et al. 2017. NLRP3 inflammasome blockade reduces liver inflammation and fibrosis in experimental NASH in mice. *Journal of hepatology* 66: 1037–1046. https://doi.org/10.1016/j.jhep.2017.01.022.
13. Green, Jack P., Yu. Shi, Fatima Martin-Sanchez, Pablo Pelegrin, Gloria Lopez-Castejon, Catherine B. Lawrence, and David Brough. 2018. Chloride regulates dynamic NLRP3-dependent ASC oligomerization and inflammasome priming. *Proceedings of the National Academy of Sciences of the United States of America* 115: E9371–E9380. https://doi.org/10.1073/pnas.1812744115.
14. Mills, Evanna L., Dylan G. Ryan, Hiran A. Prag, Dina Dikovskaya, Deepthi Menon, Zbigniew Zaslona, Mark P. Jedrychowski, Ana S H. Costa, Maureen Higgins, and Emily Hams. 2018. Itaconate is an anti-inflammatory metabolite that activates Nrf2 via alkylation of KEAP1. *Nature* 556: 113.
15. Tang, Chun, Shengyu Tan, Yiqing Zhang, Lini Dong, and Xu. Yan. 2019. Activation of Keap1-Nrf2 signaling by 4-octyl itaconate protects human umbilical vein endothelial cells from high glucose. *Biochemical and biophysical research communications* 508: 921–927. https://doi.org/10.1016/j.bbrc.2018.12.032.
16. Kim, Yong Ook, Yury Popov, and Detlef Schuppan. 2017. Optimized mouse models for liver fibrosis. *Methods in Molecular Biology* 1559: 279–296. https://doi.org/10.1007/978-1-4939-6786-5_19.
17. Dwivedi, D.K., and G.B. Jena. 2019. NLRP3 inhibitor glibenclamide attenuates high-fat diet and streptozotocin-induced non-alcoholic fatty liver disease in rat: Studies on oxidative stress inflammation DNA damage and insulin signalling pathway. *Naunyn-Schmiedeberg's Archives of Pharmacology* 393: 705–716. https://doi.org/10.1007/s00210-019-01773-5.
18. Lin, Yu-Ju, I-Chun Lin, Hong-Ren Yu, Jiunn-Ming Sheen, Li-Tung Huang, and You-Lin Tain. 2018. Early postweaning treatment with dimethyl fumarate prevents prenatal dexamethasone- and postnatal high-fat diet-induced programmed hypertension in male rat offspring. *Oxidative medicine and cellular longevity* 2018: 5343462. https://doi.org/10.1155/2018/5343462.
19. Ahmed, Danish, Vikas Kumar, Amita Verma, Manju Sharma, and Manju Sharma. 2015. Antidiabetic, antioxidant, antihyperlipidemic effect of extract of Euryale ferox salisb. With enhanced histopathology of pancreas, liver and kidney in streptozotocin induced diabetic rats. *SpringerPlus* 4:315. https://doi.org/10.1186/s40064-015-1059-7
20. Dwivedi, D.K., and G.B. Jena. 2020. Diethylnitrosamine and thioacetamide-induced hepatic damage and early carcinogenesis in rats: Role of Nrf2 activator dimethyl fumarate and NLRP3 inhibitor glibenclamide. *Biochemical and Biophysical Research Communications* 522: 381–387. https://doi.org/10.1016/j.bbrc.2019.11.100.
21. Fu, Qun, Jing Li, Lili Qiu, Jiaping Ruan, Mingjie Mao, Shuming Li, and Qinghong Mao. 2020. Inhibiting NLRP3 inflammasome with MCC950 ameliorates perioperative neurocognitive disorders suppressing neuroinflammation in the hippocampus in aged mice. *International immunopharmacology* 82: 106317. https://doi.org/10.1016/j.intimp.2020.106317.
22. Wang, Hao, Xuming Sun, Hunter S. Hodge, Carlos M. Ferrario, and Leanne Groban. 2019. NLRP3 inhibition improves heart function in GPER knockout mice. *Biochemical and biophysical research communications* 514: 998–1003. https://doi.org/10.1016/j.bbrc.2019.05.045.
23. Yi, Zhongjie, Meihong Deng, Melanie J. Scott, Fu. Guang, Patricia A. Loughran, Zhao Lei, Shilai Li, et al. 2020. IRG1/itaconate activates Nrf2 in hepatocytes to protect against liver

ischemia-reperfusion injury. *Hepatology* 72: 1394–1411. https://doi.org/10.1002/hep.31147.
24. Tian, Feng, Zhe Wang, Junqiu He, Zhihao Zhang, and Ninghua Tan. 2020. 4-Octyl itaconate protects against renal fibrosis via inhibiting TGF-beta/Smad pathway, autophagy and reducing generation of reactive oxygen species. *European journal of pharmacology* 873: 172989. https://doi.org/10.1016/j.ejphar.2020.172989.
25. Pandey, Surya Narayan, Mohit Kwatra, Durgesh Kumar Dwivedi, Priyansha Choubey, Mangala Lahkar, and Ashok Jangra. 2020. 7,8-Dihydroxyflavone alleviated the high-fat diet and alcohol-induced memory impairment: Behavioral biochemical and molecular evidence. *Psychopharmacology (Berl)* 237: 1827–1840. https://doi.org/10.1007/s00213-020-05502-2.
26. Rahman, Z., D.K. Dwivedi, and G.B. Jena. 2019. Ethanol-induced gastric ulcer in rats and intervention of tert-butylhydroquinone: Involvement of Nrf2/HO-1 signalling pathway. *Human & Experimental Toxicology* 39: 547–562. https://doi.org/10.1177/0960327119895559.
27. Ishak, K., A. Baptista, L. Bianchi, F. Callea, J. De Groote, F. Gudat, H. Denk, V. Desmet, G. Korb, and R.N. MacSween. 1995. Histological grading and staging of chronic hepatitis. *Journal of hepatology* 22: 696–699. https://doi.org/10.1016/0168-8278(95)80226-6.
28. Wang, Huafeng, Huan Zhang, Zimu Zhang, Biao Huang, Xixi Cheng, Dan Wang, Zha la Gahu, et al. 2016. Adiponectin-derived active peptide ADP355 exerts anti-inflammatory and anti-fibrotic activities in thioacetamide-induced liver injury. *Scientific Reports* 6: 19445. https://doi.org/10.1038/srep19445.
29. Chittaranjan, Sahu, Aarzoo Charaya, Shivani Singla, Durgesh K. Dwivedi, and Gopabandhu Jena. 2020. Zinc deficient diet increases the toxicity of bisphenol A in rat testis. *Journal of biochemical and molecular toxicology* 34: e22549. https://doi.org/10.1002/jbt.22549.
30. Sahu, C., D.K. Dwivedi, and G.B. Jena. 2020. Zinc and selenium combination treatment protected diabetes-induced testicular and epididymal damage in rat. *Human & experimental toxicology* 39: 1235–1256. https://doi.org/10.1177/0960327120914963.
31. Chen, Yuan-Li., Xu. Guo, Xiao Liang, Juan Wei, Jing Luo, Guan-Nan. Chen, Xiao-Di. Yan, Xue-Ping. Wen, Ming Zhong, and Xin Lv. 2016. Inhibition of hepatic cells pyroptosis attenuates CLP-induced acute liver injury. *American journal of translational research* 8: 5685–5695.
32. Abdelrahman, Rehab S., and Noha Abdel-Rahman. 2019. Dimethyl fumarate ameliorates acetaminophen-induced hepatic injury in mice dependent of Nrf-2/HO-1 pathway. *Life sciences* 217: 251–260. https://doi.org/10.1016/j.lfs.2018.12.013.
33. Wang, Jinglin, Haozhen Ren, Xianwen Yuan, Hucheng Ma, Xiaolei Shi, and Yitao Ding. 2018. Interleukin-10 secreted by mesenchymal stem cells attenuates acute liver failure through inhibiting pyroptosis. *Hepatology research: The official journal of the Japan Society of Hepatology* 48: E194–E202. https://doi.org/10.1111/hepr.12969.
34. de David, Cintia, Graziella Rodrigues, Silvia Bona, Luise Meurer, Javier Gonzalez-Gallego, Maria Jesus Tunon, and Norma Possa Marroni. 2011. Role of quercetin in preventing thioacetamide-induced liver injury in rats. *Toxicologic pathology* 39: 949–957. https://doi.org/10.1177/0192623311418680.
35. Kapoor, Radhika, and Poonam Kakkar. 2014. Naringenin accords hepatoprotection from streptozotocin induced diabetes in vivo by modulating mitochondrial dysfunction and apoptotic signaling cascade. *Toxicology reports* 1: 569–581. https://doi.org/10.1016/j.toxrep.2014.08.002.
36. Schupp, Nicole, Reinhard Schinzel, August Heidland, and Helga Stopper. 2005. Genotoxicity of advanced glycation end products: Involvement of oxidative stress and of angiotensin II type 1 receptors. *Annals of the New York Academy of Sciences* 1043: 685–695. https://doi.org/10.1196/annals.1333.079.
37. Ma, Xingyu, Yang Zhou, Bingke Qiao, Songhong Jiang, Qian Shen, Yuzhu Han, Anfang Liu, et al. 2020. Androgen aggravates liver fibrosis by activation of NLRP3 inflammasome in CCl4 induced liver injury mouse model. *American Journal of Physiology-Endocrinology and Metabolism* 318: E817–E829. https://doi.org/10.1152/ajpendo.00427.2019.
38. Wree, Alexander, Akiko Eguchi, Matthew D. McGeough, Carla A. Pena, Casey D. Johnson, Ali Canbay, Hal M. Hoffman, and Ariel E. Feldstein. 2014. NLRP3 inflammasome activation results in hepatocyte pyroptosis liver inflammation and fibrosis in mice. *Hepatology* 59: 898–910. https://doi.org/10.1002/hep.26592.
39. Watanabe, Azuma, Muhammad Adnan Sohail, Dawidson Assis Gomes, Ardeshir Hashmi, Jun Nagata, Fayyaz Shiraz Sutterwala, Shamail Mahmood, et al. 2009. Inflammasome-mediated regulation of hepatic stellate cells. *American journal of physiology Gastrointestinal and Liver Physiology* 296: G1248–G1257. https://doi.org/10.1152/ajpgi.90223.2008.
40. Boaru, Sorina Georgiana, Erawan Borkham-Kamphorst, Eddy Van de Leur, Eric Lehnen, Christian Liedtke, and Ralf Weiskirchen. 2015. NLRP3 inflammasome expression is driven by NF-kappaB in cultured hepatocytes. *Biochemical and biophysical research communications* 458: 700–706. https://doi.org/10.1016/j.bbrc.2015.02.029.
41. Arriola Benitez, Paula Constanza, Ayelen Ivana Pesce Viglietti, Marco Tulio R. Gomes, Sergio Costa Oliveira, Jorge Fabian Quarleri, Guillermo Hernan Giambartolomei, and Maria Victoria Delpino. 2019. Brucella abortus infection elicited hepatic stellate cell-mediated fibrosis through inflammasome-dependent IL-1beta production. *Frontiers in immunology* 10: 3036. https://doi.org/10.3389/fimmu.2019.03036.
42. Garstkiewicz, Martha, Gerhard E. Strittmatter, Serena Grossi, Jennifer Sand, Gabriele Fenini, Sabine Werner, Lars E. French, and Hans-Dietmar. Beer. 2017. Opposing effects of Nrf2 and Nrf2-activating compounds on the NLRP3 inflammasome independent of Nrf2-mediated gene expression. *European journal of immunology* 47: 806–817. https://doi.org/10.1002/eji.201646665.
43. Miglio, Gianluca, Eleonora Veglia, and Roberto Fantozzi. 2015. Fumaric acid esters prevent the NLRP3 inflammasome-mediated and ATP-triggered pyroptosis of differentiated THP-1 cells. *International immunopharmacology* 28: 215–219. https://doi.org/10.1016/j.intimp.2015.06.011.
44. Giustina, Amanda Della, Sandra Bonfante, Graciela Freitas Zarbato, Lucineia Gainski Danielski, Khiany Mathias, Aloir Neri Jr de Oliveira, Leandro Garbossa, et al. 2018. Dimethyl fumarate modulates oxidative stress and inflammation in organs after sepsis in rats. *Inflammation* 41:315-327. https://doi.org/10.1007/s10753-017-0689-z
45. Zhang, Ning-Ping., Xue-Jing. Liu, Li. Xie, Xi-Zhong. Shen, and Wu. Jian. 2019. Impaired mitophagy triggers NLRP3 inflammasome activation during the progression from nonalcoholic fatty liver to nonalcoholic steatohepatitis. *Laboratory investigation: A journal of technical methods and pathology* 99: 749–763. https://doi.org/10.1038/s41374-018-0177-6.
46. Liao, Shan-Ting., Chao Han, Xu. Ding-Qiao, Fu. Xiao-Wei, Jun-Song. Wang, and Ling-Yi. Kong. 2019. 4-Octyl itaconate inhibits aerobic glycolysis by targeting GAPDH to exert anti-inflammatory

effects. *Nature communications* 10: 5091. https://doi.org/10.1038/s41467-019-13078-5.
47. Dwivedi, D.K., and G.B. Jena. 2018. Glibenclamide protects against thioacetamide-induced hepatic damage in Wistar rat: Investigation on NLRP3 MMP-2 and stellate cell activation. *Naunyn-Schmiedeberg's Archives of Pharmacology* 391: 1257–1274. https://doi.org/10.1007/s00210-018-1540-2.
48. Schulze-Topphoff, Ulf, Michel Varrin-Doyer, Kara Pekarek, Collin M. Spencer, Aparna Shetty, Sharon A. Sagan, Bruce A. C. Cree, et al. 2016. Dimethyl fumarate treatment induces adaptive and innate immune modulation independent of Nrf2. *Proceedings of the National Academy of Sciences of the United States of America* 113: 4777–4782. https://doi.org/10.1073/pnas.1603907113.